RNA (2001), *7*:194–206. Cambridge University Press. Printed in the USA.

Mechanism of ribosome recruitment by hepatitis C IRES RNA

JEFFREY S. KIEFT,[1] KAIHONG ZHOU,[1] RONALD JUBIN,[2] and JENNIFER A. DOUDNA[1]

[1]Department of Molecular Biophysics and Biochemistry and Howard Hughes Medical Institute, Yale University, New Haven, Connecticut 06520-8114, USA
[2]Schering-Plough Research Institute, Kenilworth, New Jersey 07033-0539, USA

ABSTRACT

Many viruses and certain cellular mRNAs initiate protein synthesis from a highly structured RNA sequence in the 5′ untranslated region, called the internal ribosome entry site (IRES). In hepatitis C virus (HCV), the IRES RNA functionally replaces several large initiation factor proteins by directly recruiting the 43S particle. Using quantitative binding assays, modification interference of binding, and chemical and enzymatic footprinting experiments, we show that three independently folded tertiary structural domains in the IRES RNA make intimate contacts to two purified components of the 43S particle: the 40S ribosomal subunit and eukaryotic initiation factor 3 (eIF3). We measure the affinity and demonstrate the specificity of these interactions for the first time and show that the high affinity interaction of IRES RNA with the 40S subunit drives formation of the IRES RNA•40S•eIF3 ternary complex. Thus, the HCV IRES RNA recruits 43S particles in a mode distinct from both eukaryotic cap-dependent and prokaryotic ribosome recruitment strategies, and is architecturally and functionally unique from other large folded RNAs that have been characterized to date.

Keywords: 40S subunit; eIF3; internal ribosome entry site (IRES); RNA structure; translation initiation

INTRODUCTION

Eukaryotic cells and their viruses have evolved at least two mechanisms for recruiting and positioning ribosomes at the start sites for translation of RNA messages. The primary mechanism involves recognition of a 7-methyl guanosine cap on the 5′ terminus of the mRNA by a set of canonical initiation factors that recruit the 43S particle—including the 40S ribosomal subunit and eukaryotic initiation factor 3 (eIF3)—forming the 48S preinitiation complex (Fig. 1A; for review, see Merrick & Hershey, 1996; Pain, 1996; Sachs et al., 1997). Alternatively, numerous viruses and some eukaryotic mRNAs utilize a cap-independent pathway in which an RNA element, the internal ribosome entry site (IRES), drives preinitiation complex formation by positioning the ribosome on the message, either at or just upstream of the start site. In hepatitis C virus (HCV), the major infectious agent leading to non-A, non-B hepatitis, the minimum IRES includes nearly the entire 5′ untranslated region (UTR) of the message (for review, see Rijnbrand & Lemon, 2000). The secondary structure of the HCV IRES RNA, one of the most conserved regions of the entire viral genome, is critical for translation initiation, and is similar to that of the related pestiviruses and GB virus B (Brown et al., 1992; Wang et al., 1994, 1995; Le et al., 1995; Rijnbrand et al., 1995; Honda et al., 1996a, 1996b, 1999; Pickering et al., 1997; Varaklioti et al., 1998; Psaridi et al., 1999; Tang et al., 1999).

We have previously shown that the HCV IRES RNA adopts a specific three-dimensional fold in the presence of physiological concentrations of metal ions (Kieft et al., 1999). Rather than forming a tightly packed globular structure, the RNA helices extend from two folded helical junctions, JIIIabc and JIIIef (Fig. 1B). This suggests that the IRES RNA acts as a structural scaffold in which specifically placed recognition sites recruit the translational machinery. This is supported by the observation that eIF3 and the 40S ribosomal subunit, the two largest components of the 43S particle, bind directly to the HCV IRES RNA (Pestova et al., 1998). Unlike IRESs found in some other RNA viruses, such as poliovirus, the IRES RNA•40S•eIF3 ternary pre-

Reprint requests to: Jennifer A. Doudna, Department of Molecular Biophysics and Biochemistry and Howard Hughes Medical Institute, Yale University, New Haven, Connecticut 06520-8114, USA; e-mail: doudna@csb.yale.edu.

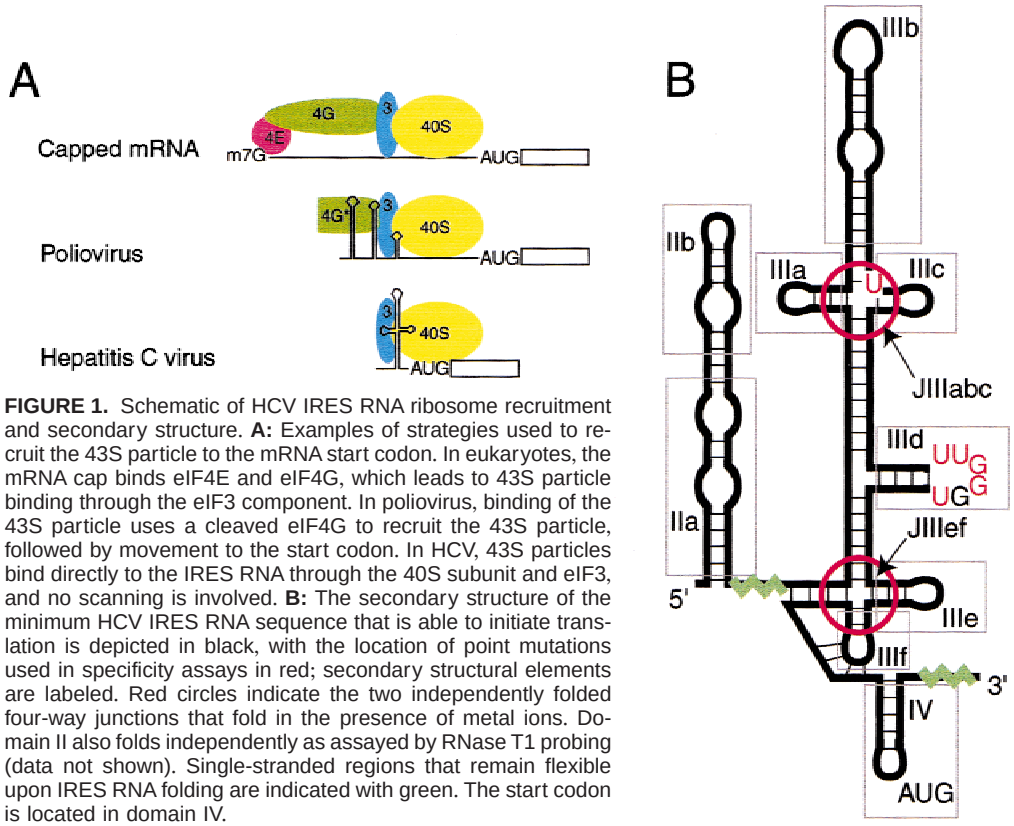

FIGURE 1. Schematic of HCV IRES RNA ribosome recruitment and secondary structure. **A:** Examples of strategies used to recruit the 43S particle to the mRNA start codon. In eukaryotes, the mRNA cap binds eIF4E and eIF4G, which leads to 43S particle binding through the eIF3 component. In poliovirus, binding of the 43S particle uses a cleaved eIF4G to recruit the 43S particle, followed by movement to the start codon. In HCV, 43S particles bind directly to the IRES RNA through the 40S subunit and eIF3, and no scanning is involved. **B:** The secondary structure of the minimum HCV IRES RNA sequence that is able to initiate translation is depicted in black, with the location of point mutations used in specificity assays in red; secondary structural elements are labeled. Red circles indicate the two independently folded four-way junctions that fold in the presence of metal ions. Domain II also folds independently as assayed by RNase T1 probing (data not shown). Single-stranded regions that remain flexible upon IRES RNA folding are indicated with green. The start codon is located in domain IV.

initiation complex forms without the involvement of other cellular factors (Fig. 1A; Pestova et al., 1998). Although several other proteins appear to interact with the HCV IRES RNA, they are not required for 43S binding to the IRES (Ali & Siddiqui, 1995, 1997; Yen et al., 1995; Hahm et al., 1998; Fukushi et al., 1999). Direct binding of the small ribosomal subunit to the mRNA is also observed in prokaryotes, in which binding is largely governed by 16S rRNA base pairing to the short (~2–10 nt) Shine–Dalgarno sequence (Shine & Dalgarno, 1974).

How does the HCV IRES RNA tertiary structure recognize, bind, and position the translational machinery, tasks that normally require several other large protein initiation factors? Although the approximate binding sites of the 40S ribosomal subunit and eIF3 have been mapped onto the HCV IRES secondary structure, the identities and contributions of the RNA tertiary structures involved in forming these sites have not been elucidated (Buratti et al., 1998; Pestova et al., 1998; Sizova et al., 1998; Kolupaeva et al., 2000; Odreman-Macchioli et al., 2000). An understanding of the mechanism of cap-independent translation requires knowledge of the contributions of each IRES RNA tertiary structural domain to 43S particle binding as well as to downstream events. Using purified components in quantitative biochemical and structural experiments, we demonstrate that the multiple independent domains of the HCV IRES RNA tertiary structure work synergistically to specifically recognize both eIF3 and the 40S ribosomal subunit. One of these domains, a folded four-way junction, makes contact with both the 40S subunit and eIF3 and thus must lay at the interface between these two components of the 43S particle. Translation initiation assays and direct binding measurements of both wild-type and mutant HCV IRES RNAs suggest that recruitment of the 43S particle to the HCV message is driven through the high affinity HCV IRES RNA•40S interaction, involving a novel strategy of ribosome recruitment distinct from both eukaryotic cap-dependent and prokaryotic mechanisms.

RESULTS

Affinity and specificity of the HCV IRES RNA binding to 43S particle components

To measure the affinity of the HCV IRES RNA for the 40S subunit, radiolabeled IRES RNA prepared by in vitro transcription was incubated with purified rabbit 40S subunits and the resulting complexes were quantitated by filter binding. The HCV IRES RNA binds the 40S subunit with an apparent equilibrium dissociation constant (K_d) of 1.9 ± 0.3 nM (Fig. 2A). In contrast, the IRES RNA was unable to bind purified archaeal 30S subunits from *Haloarcus marismortui* under any of a

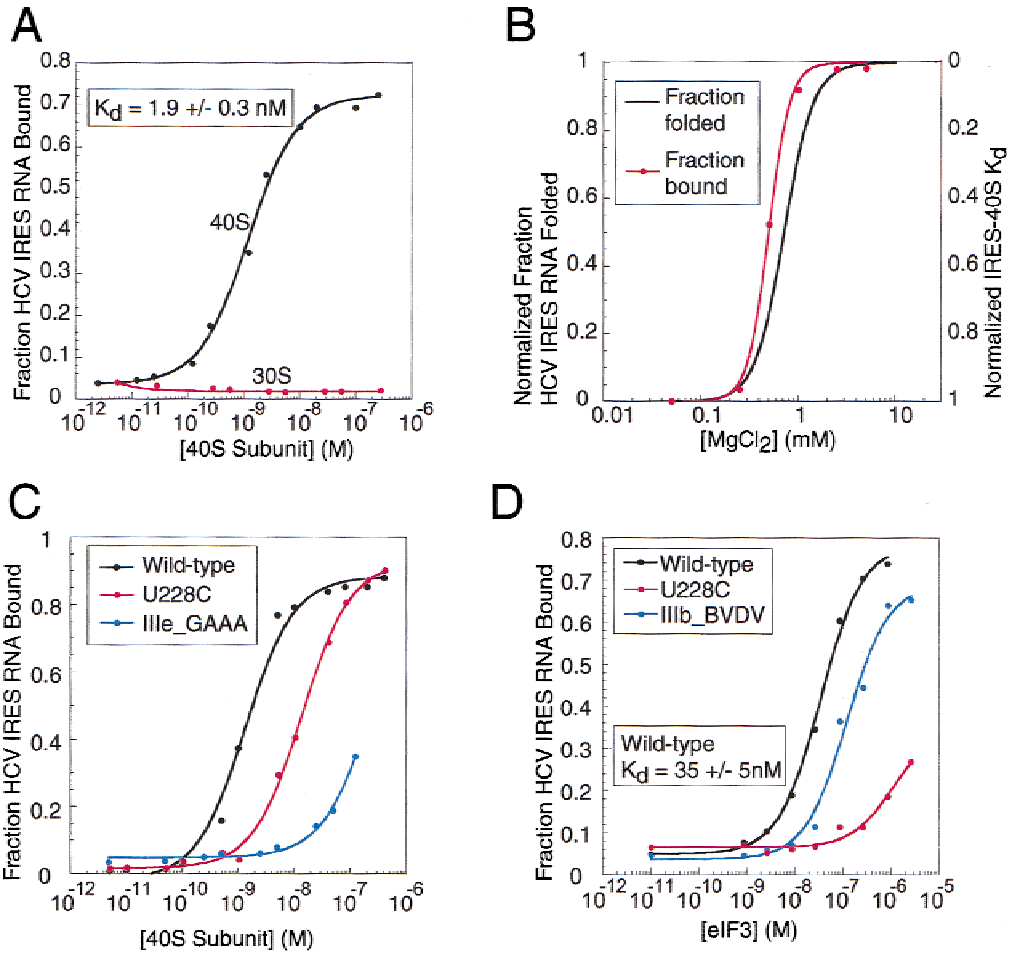

FIGURE 2. Binding of wild-type and mutant HCV IRES RNAs to components of the 43S particle. **A**: Binding isotherm of wild-type HCV IRES RNA to purified 40S subunits and *H. marismortui* 30S subunits. **B**: Magnesium dependence of the K_d of IRES RNA•40S complex formation is plotted in red; the curve for IRES RNA folding as a function of magnesium ion concentration is plotted in black (for clarity, the data points for the fraction folded curve have been omitted; Kieft et al., 1999). **C**: Binding isotherms of wild-type and mutant IRES RNAs to 40S subunit. Binding reactions required 250–300 mM KCl to eliminate nonspecific RNA binding to the 40S subunit; spermidine or tRNA was not as effective for that purpose. **D**: Binding isotherms of wild-type and mutant IRES RNAs to purified eIF3.

variety of salt conditions. We also verified the 1:1 ratio of the IRES RNA•40S complex using stoichiometric binding assays (data not shown). Because previous experiments demonstrated that IRES RNA folding requires less than 1 mM magnesium ion, we measured the K_d of the IRES RNA•40S complex as a function of magnesium ion concentration (Fig. 2B). Binding is almost nonexistent in the absence of added magnesium, but increases with increasing magnesium ion concentration up to ~2 mM. The magnesium ion dependence of IRES RNA•40S complex formation is very similar to that for IRES RNA tertiary structure formation and for maximal HCV IRES driven translation initiation in vitro (Borman et al., 1995; Kieft et al., 1999). This result suggests that binding of the 40S subunit to the IRES RNA and subsequent translation initiation requires the formation of the magnesium-induced IRES tertiary structure, although magnesium-dependent ribosome stability may also play a role.

To explore the specificity of the IRES RNA•40S interaction, we measured the affinity of the 40S subunit for HCV IRES RNA point mutants that have been previously characterized in terms of folding and in vitro translation initiation activity (Kieft et al., 1999). Point mutations in loop IIId (U264A, U265A, U269A, G266C, and G267C) have been shown to affect both secondary structure formation and in vitro translation initiation activity (Fig. 1B). Mutations of the uracils within loop IIId that do not change the RNA secondary structure, as assayed by RNase T1 probing (data not shown), have an intermediate effect on IRES activity, and do not affect 40S subunit binding (Table 1). However, mutations of guanosines in loop IIId have stronger deleterious effects on both translation initiation and 40S subunit binding, and in the case of G266C, alter the ion-dependent structure of the RNA (Kieft et al., 1999). A single mutation at U228 that prevents the folding of junction JIIIabc (U228C) initiates translation at only 5%

TABLE 1. Translation initiation activities and 40S binding affinity for wild-type HCV IRES RNA and various point mutants.

RNA sequence	Translation activity[a] (%)	K_d—Binding to 40S (nM)	K_d—Binding to eIF3 (nM)
Wild-type	100	1.9 ± 0.4	35 ± 5
Loop IIId point mutants			
U264A	13[b]	2.2 ± 1.1	n.d.[c]
U265A	50[b]	2.0 ± 0.4	n.d.
G266C	3[b]	9.5 ± 2.7	n.d.
G267C	2[b]	8.7 ± 1.0	n.d.
U269A	40[b]	2.9 ± 0.2	n.d.
JIIIabc point mutant			
U228C	5[b]	11.7 ± 4.8	>500

[a]Activity is reported as percentage of wild-type translation initiation activity.
[b]Previously reported value (Kieft et al., 1999).
[c]n.d.: not done.

of the wild-type level and binds the 40S subunit about fivefold less tightly than wild-type IRES RNA (Table 1). The sensitivity of the IRES RNA•40S interaction to IRES RNA point mutations is the first rigorous, quantitative demonstration that this interaction is driven by specific intermolecular contacts between accessible ribosomal surfaces and IRES RNA functional groups, rather than by nonspecific 40S subunit affinity for RNA.

The other component of the 43S particle that binds to the HCV IRES RNA is eIF3, a multisubunit protein complex of over 600 kDa. To analyze affinity and specificity of purified eIF3 binding to the HCV IRES RNA, we conducted filter binding experiments under conditions identical to those used to analyze 40S subunit binding. The K_d of IRES RNA•eIF3 complex formation is 35 ± 5 nM, more than 15-fold above the K_d for the IRES RNA•40S complex (Fig. 2D). Because eIF3 contains an inherent mRNA binding activity (Garcia-Barrio et al., 1995), we tested the specificity of this recognition event by measuring the affinity of eIF3 for the IRES RNA sequence that contains the mutation U228C. This mutant displays reduced affinity for eIF3 (Fig. 2D), with U228C having a $K_d > 500$ nM, at least 15 times greater than wild type. Like the 40S subunit interaction, eIF3 binding to the IRES is sensitive to a point mutation and is thus highly specific.

IRES RNA structural determinants of IRES RNA•40S complex formation

The elements of the IRES RNA secondary and tertiary structure that confer 40S subunit affinity and specificity were identified using a combination of footprinting and modification interference experiments. To determine the footprint of specifically bound 40S subunit on the IRES RNA, we probed the complex using ribonuclease (RNase) T1 and phosphorothioate footprinting. Upon folding, recognition loops in the IRES RNA remain sensitive to cleavage by RNase T1 (Kieft et al., 1999). In the presence of bound 40S subunits, these cleavage sites in loops IIb, IIIa, IIId, and domain IV are substantially protected (Fig. 3A,D). A recent enzymatic footprinting analysis of 40S subunit binding to the HCV IRES RNA identified domains IIId and IV as contact points for the 40S subunit, but did not identify loops IIb and IIIa (Kolupaeva et al., 2000). To probe the entire RNA, independent of sequence or secondary structure, we used iodine cleavage of HCV IRES RNA molecules that were transcribed with 5% incorporation of phosphorothioate linkages (Christian & Yarus, 1992). Binding of the 40S subunit protects portions of the IRES RNA backbone from solvent access (Fig. 3B,D). The phosphorothioate footprint includes stems, internal loops, and hairpin loops in domains IIb, IIIa, IIIc, IIId, IIIe, IIIf, and IV, but not domain IIIb or IIa, demonstrating extensive and intimate association of the IRES and the 40S subunit (Fig. 3D).

Footprinting identifies areas of intermolecular contact, but does not yield information about which nucleotides within the footprint determine binding affinity. To address this, we used modification interference, a technique in which functional RNAs are selected from a pool of randomly modified molecules (Conway & Wickens, 1989). Radiolabeled HCV IRES RNA was modified with diethylpyrocarbonate (DEPC), which ethylates adenosine bases at the N7 position, to produce a pool of molecules in which each RNA contained, on average, one modified adenosine. This RNA was incubated with 40S subunits and the bound IRES RNA was recovered and analyzed to identify locations where modification interferes with 40S subunit binding. This analysis reveals that adenosine bases involved in 40S subunit recognition are clustered around JIIIef and loop IIIa (Fig. 3C,D). Loop IIIa is not involved in forming the ion-induced fold of the IRES RNA as assayed by RNase T1 probing (data not shown); thus it may represent a specific recognition element for the IRES RNA•40S interaction. Loop IIIe bases are protected from RNase T1 by the ion-induced fold of the RNA; thus modifying these bases may affect folding or disrupt a direct contact to the 40S subunit (Kieft et al., 1999). Adenosine bases located in both helices of a proposed pseudoknot (IIIf; Fig. 1B) may also be important for stabilizing this tertiary interaction or for directly interacting with the 40S subunit. No critical adenosine residues were identified in domains II, IIIb, or IV, indicating that while these regions are proximal to the 40S subunit, they do not contain adenosines whose modification affects 40S subunit recognition. Apical loops IIIc and IIId are included in the 40S subunit footprint, but as they do not contain adenosine residues, their participation in binding cannot be assessed by DEPC modification.

The footprinting and modification interference results roughly identify which portions of the HCV RNA are involved in binding the 40S subunit. We next con-

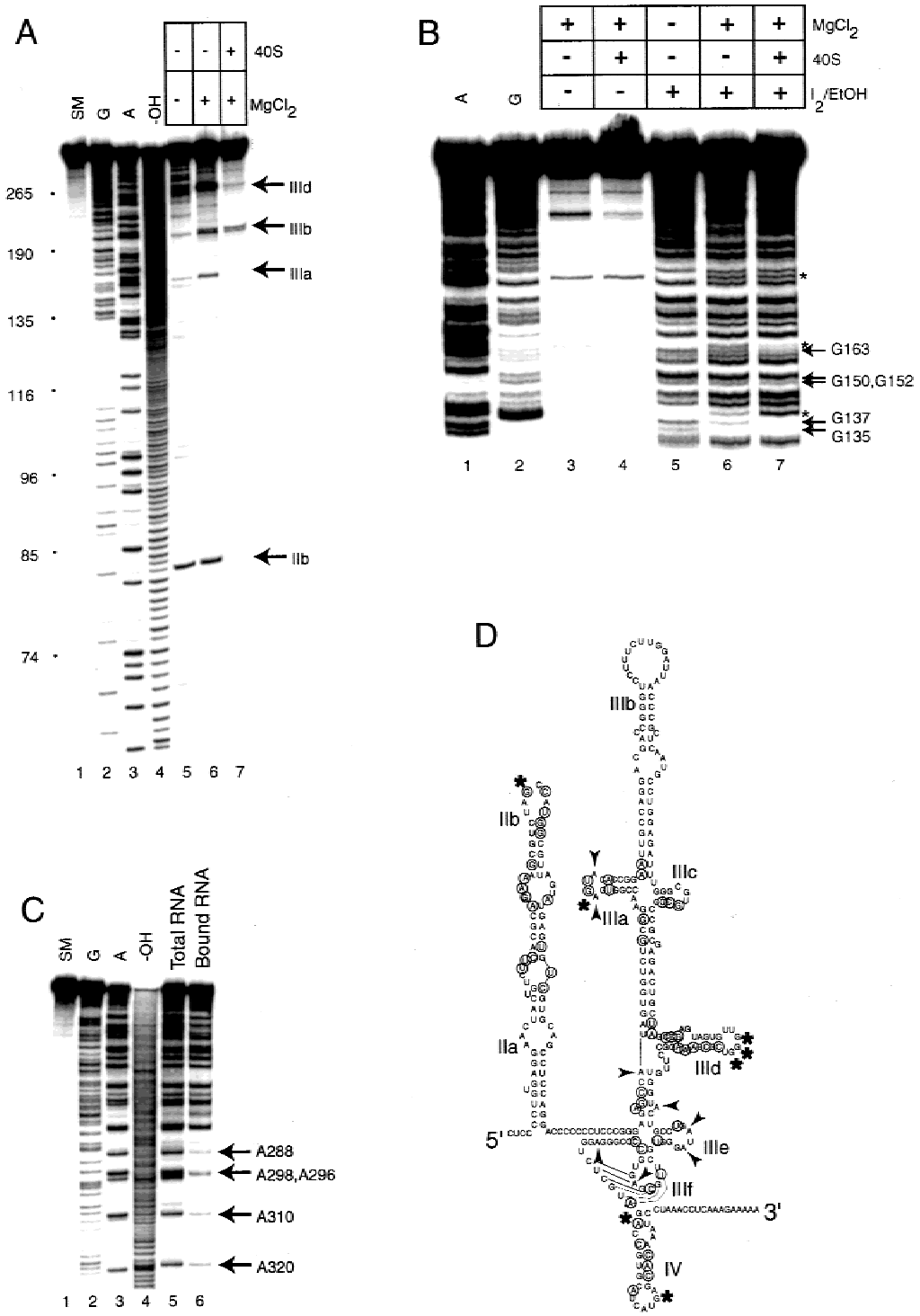

FIGURE 3. Footprinting and modification interference of binding of the IRES RNA-40S subunit complex. **A**: RNase T1 footprinting of the HCV IRES RNA with bound 40S subunit. RNase T1 cuts after guanosine residues in single-stranded RNA. Lane 5 contains RNA without added magnesium, lane 6 contains folded RNA, and lane 7 contains folded RNA with bound 40S subunit. The location of various secondary structural domains and their associated cleavage sites are shown with arrows. IIId, IIIa, and IIb are among those loops that are protected. **B**: Portion of one gel from thiophosphate footprinting of 40S subunit onto the HCV IRES RNA, using α-thio-G. Lanes 1 and 2 contain RNase U2 and T1 sequencing reactions, lanes 3 and 4 contain RNA that was not treated with molecular iodine. Lane 5 contains RNA that was denatured and immediately treated with iodine to yield a thiophosphate-G sequencing lane. The footprint is observed by comparing the subtle protections observed in lane 7 with lane 6. Examples of sites of protection are labeled with arrows; sites of background degradation are indicated with asterisks. Reported sites of protection were observed in multiple experimental repetitions. Typical protection factors were between 1.5 and 3. **C**: Portion of a DEPC modification interference of 40S binding to the HCV IRES RNA experimental gel. Lane 1 contains starting material, lanes 2 and 3 are RNase sequencing reactions, and lane 4 is a partial alkaline hydrolysis ladder. Interferences are observed by comparing lanes 5 and 6; sites of interference are indicated with arrows. **D**: Summary of footprinting and modification interference data. In the presence of bound 40S subunits, sites that were protected from RNase T1 are indicated with asterisks, sites protected from iodine cleavage are circled, and adenosine nucleotides implicated by modification interference are shown with arrows.

structed a series of IRES sequences with mutated apical loops to quantitate the thermodynamic contribution of each IRES RNA stem-loop to complex formation (Fig. 4A). In several cases, the apical loops were mutated to both their Watson–Crick complements and to an ultrastable GAAA tetraloop, to control for secondary structural changes or binding effects unique to one type of mutant. Mutants IIIc_GAAA, IIIb_BVDV, and IIIa_comp were probed with RNase T1 to verify that they did not alter the ion-induced fold (data not shown). As predicted, mutations in stem-loops identified by modification interference (IIIa and IIIe) caused a reduction in binding affinity, as did mutations in other loops within the 40S subunit footprint (IIIc, IIId; Table 2). Translation initiation activity of these mutants correlates with ability to bind to the 40S subunit, as they are all severely inhibited. The loop IIIb mutant bound with wild-type affinity, and also was able to initiate translation at 50% of wild-type activity.

Loop IIIf is proposed to form a pseudoknot by base pairing to nucleotides just upstream of the stem-loop that contains the start codon (domain IV; Wang et al., 1995). To explore the possible role of this structure in preinitiation complex formation, we prepared a series of pseudoknot mutants (Fig. 4B), and measured their 40S subunit binding ability. Abrogation of the potential pseudoknot interaction by mutation of either nt 325–330 or by mutation of loop IIIf results in a two- to threefold reduction in 40S subunit binding affinity (Table 2), yet IRES translation initiation activity is lost. A somewhat stronger effect is observed with mutants in which the potential pseudoknot interaction is partially or fully restored through compensatory mutations (Fig. 4B).

TABLE 2. Translation initiation activity, 40S subunit binding affinity, and eIF3 binding affinity of HCV IRES stem-loop and pseudoknot mutants.

RNA sequence	Translation activity[a] (%)	K_d—Binding to 40S (nM)	K_d—Binding to eIF3 (nM)
Stem-loop mutants			
IIIa_comp	<10	13.1 ± 1.5	>200
IIIb_BVDV	50	1.2 ± 0.1	120
IIIc_comp	20	14.5 ± 0.5	40
IIIc_GAAA	<10	24 ± 6.2	36
G(266-268)C	2[b]	>50	n.d.[c]
IIIe_comp	<10	>50	n.d.
IIIe_GAAA	<10	>50	37
IIIf/Pseudoknot mutants			
IIIf+stem_comp	<1	11.8 ± 5.5	37
IIIf_comp	<10	3.8 ± 1.0	n.d.
IIIf_GAAA	<10	4.1 ± 0.9	n.d.
325-330_comp	<10	4.5 ± 1.2	n.d.
Pknot_δrestore	<10	8.2 ± 3.5	n.d.
Pknot_restore	<10	5.2 ± 1.0	n.d.

[a]Activity is reported as percentage of wild-type translation initiation activity.
[b]Previously reported (Kieft et al., 1999).
[c]n.d.: not done.

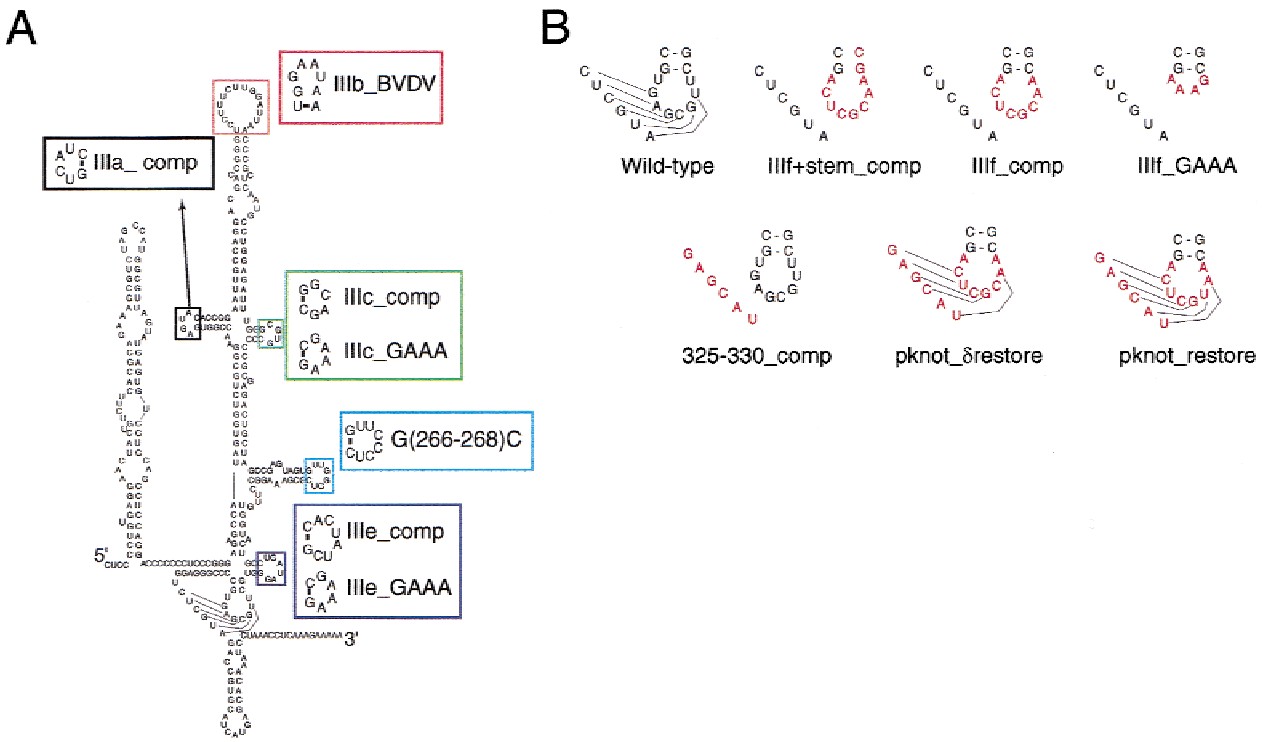

FIGURE 4. Apical loop pseudoknot mutants. **A**: The sequences and names of apical loop mutants used in binding experiments are shown. **B**: The sequences and names of pseudoknot mutants are shown, with the mutated nucleotides in red.

When the IIIf loop is mutated and the IIIf stem is also destabilized, 40S subunit affinity decreases more significantly to mirror the significant loss of translation initiation activity. Therefore, although mutations to the proposed pseudoknot strongly inhibit translation initiation activity, they have more modest effects on ribosomal subunit binding when compared to mutations in other IRES RNA elements, such as loop IIIe or loop IIId. This result suggests that the sequence of the RNA involved in the putative pseudoknot is more important than the pseudoknot interaction itself for binding the 40S subunit. It is also possible that the proposed IIIf pseudoknot does not form as drawn, or that its formation is important for driving events downstream of 43S binding, such as correct positioning of domain IV on the ribosome, rather than purely for ribosome recognition by the IRES.

IRES RNA structural determinants of IRES RNA•eIF3 complex formation

Modification interference experiments analogous to those described above were used to identify nucleotides critical for eIF3 binding to the IRES RNA. The IRES RNA was treated with DEPC or with aqueous hydrazine to modify adenosine and guanosine residues, or uracil residues, respectively. These experiments implicated nucleotides in the apical and internal loops of domain IIIb, in stem-loop IIIa, and in junction IIIabc in binding of the IRES to eIF3 (Fig. 5,B). The energetic contributions of individual IRES stem-loops to eIF3 binding were measured using IRES RNAs containing mutations in loops IIIa, IIIb, IIIc, IIIe, or IIIf (Fig. 4A,B). Consistent with the modification interference results, only mutations in loops IIIa and IIIb were deleterious to eIF3 binding; the other stem-loop mutants bound with near wild-type affinity (Table 2). This confirms that loop IIIa is a major determinant of eIF3 binding, whereas loop IIIc is not.

Identification of truncated binding structures for the 40S subunit and eIF3

The results presented above suggest that recognition of individual components of the 43S particle by the IRES RNA requires, in each case, only a subset of the entire RNA structure. To identify minimized RNA structures that bind eIF3 and the 40S ribosomal subunit, we measured the binding affinity of the 40S subunit and eIF3 to a series of IRES RNAs with systematic domain deletions. In each case, the structure of the uncomplexed RNA was probed with either Fe(II)-EDTA or RNase T1 to verify correct ion-induced folding (Celander & Cech, 1991; Latham & Cech, 1989; Kieft et al., 1999; data not shown). As each domain was deleted, binding remained close to the wild-type level until a critical domain was removed, resulting in a dramatic decrease in affinity (Fig. 6A). For eIF3 binding, this threshold is the removal of stem-loop IIIb, and for the 40S subunit, it is the removal of junction IIIabc. Thus, the minimum binding site for eIF3 must include loop IIIb and junction IIIabc, whereas that for the 40S subunit includes both folded four-way junctions. These truncated binding sequences contain all of the domains and nucleotides we identified by footprinting, modification interference, and mutagenesis.

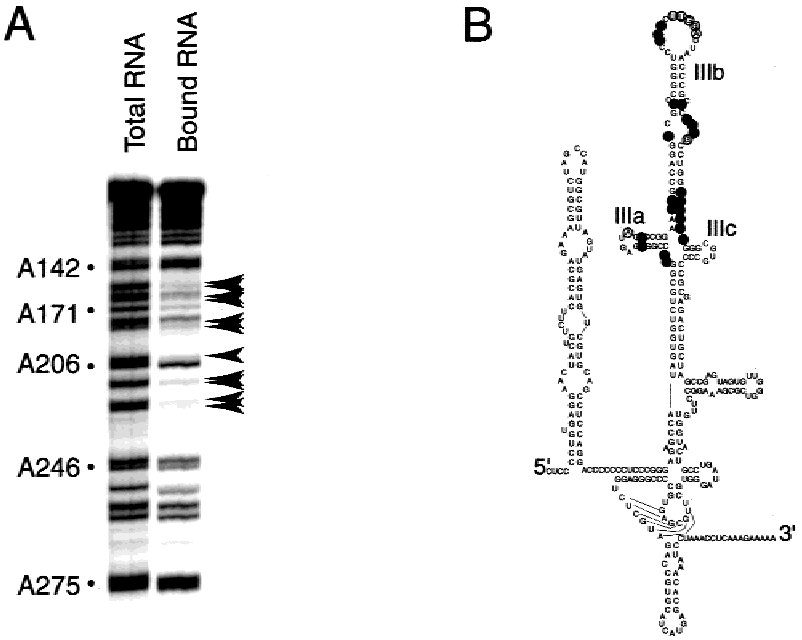

FIGURE 5. Binding of eIF3 to the HCV IRES RNA. **A**: Portion of a DEPC modification interference polyacrylamide gel used to locate nucleotides critical for eIF3 binding. Examples of interference sites are indicated with arrows. **B**: Critical nucleotides identified by DEPC and aqueous hydrazine modification interference of eIF3 binding are shown as filled circles on the IRES secondary structure. Open circles indicate weaker interference sites.

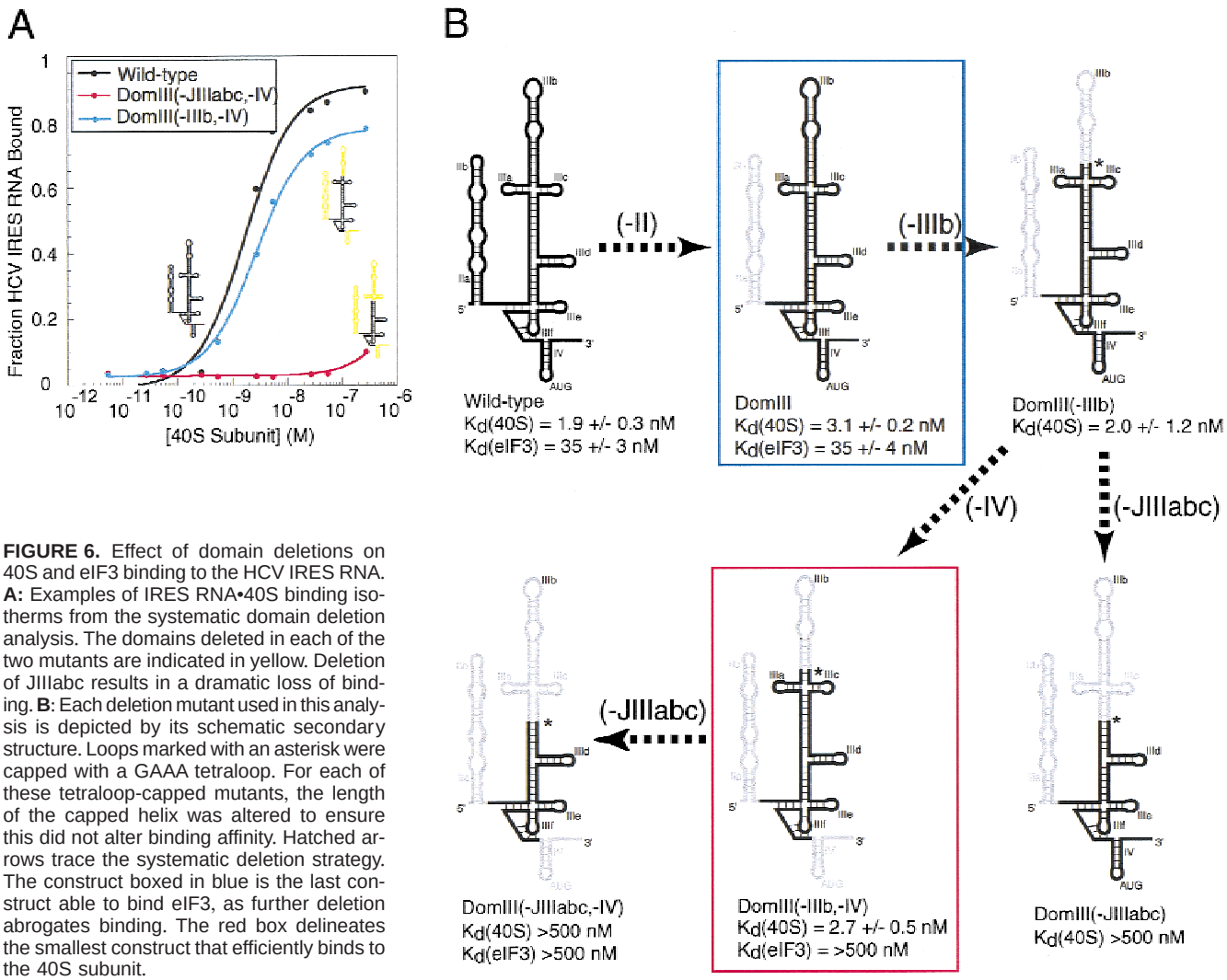

FIGURE 6. Effect of domain deletions on 40S and eIF3 binding to the HCV IRES RNA. **A:** Examples of IRES RNA•40S binding isotherms from the systematic domain deletion analysis. The domains deleted in each of the two mutants are indicated in yellow. Deletion of JIIIabc results in a dramatic loss of binding. **B**: Each deletion mutant used in this analysis is depicted by its schematic secondary structure. Loops marked with an asterisk were capped with a GAAA tetraloop. For each of these tetraloop-capped mutants, the length of the capped helix was altered to ensure this did not alter binding affinity. Hatched arrows trace the systematic deletion strategy. The construct boxed in blue is the last construct able to bind eIF3, as further deletion abrogates binding. The red box delineates the smallest construct that efficiently binds to the 40S subunit.

Binding of the 40S•eIF3 complex to the HCV IRES RNA

Analogous to the recruitment of the 43S particle in cap-dependent translation, the HCV IRES RNA probably recognizes the assembled 40S•eIF3 complex in vivo. To replicate this event, we measured the affinity of preformed 40S•eIF3 complex for wild-type HCV IRES RNA. The K_d for ternary complex formation was ~1.0 nM, virtually identical to the K_d for IRES RNA•40S complex formation (Fig. 7A). The 40S subunit and eIF3 bind to each other within the wheat germ 43S complex with a K_d of 5 nM (Goss & Rounds, 1988); assuming a similar K_d for mammalian factors, IRES binding to the 40S•eIF3 complex is as tight as interactions within the 43S particle. Furthermore, our data imply that binding of the IRES RNA to the assembled 43S particle may not be appreciably tighter than binding of the IRES to the isolated 40S subunit.

DISCUSSION

Recruitment of the 43S particle, which contains eIF3, the 40S ribosomal subunit, and a ternary eIF2•GTP•tRNA complex, to messenger RNAs is a critical step in the eukaryotic translation initiation pathway. The hepatitis C viral message, like those of some other viruses and certain cellular genes, circumvents the requirement for the 7-methyl guanosine cap by use of a structured IRES RNA in the 5′ UTR. In HCV, IRES binding to the 43S particle involves direct contacts with eIF3 and the 40S subunit (Fig. 1A). We have shown that the IRES RNA responsible for this direct interaction forms a specific three-dimensional structure that is required for translation initiation (Kieft et al., 1999). Binding of the 40S ribosomal subunit and eIF3 to the IRES, measured here using purified components, is highly specific: 30S ribosomal subunits are unable to form complexes, and certain IRES RNA point mutations in-

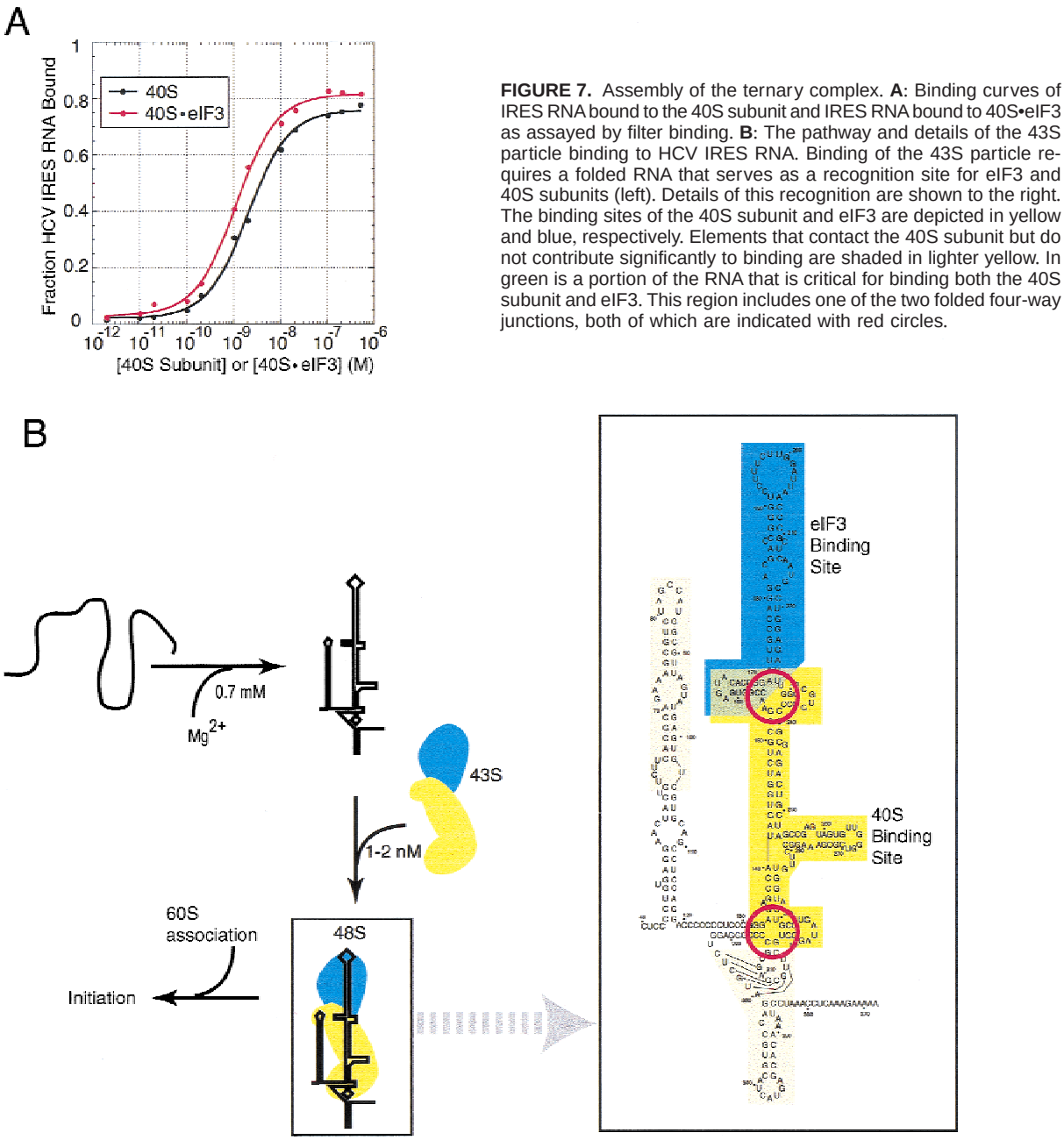

FIGURE 7. Assembly of the ternary complex. **A**: Binding curves of IRES RNA bound to the 40S subunit and IRES RNA bound to 40S•eIF3 as assayed by filter binding. **B**: The pathway and details of the 43S particle binding to HCV IRES RNA. Binding of the 43S particle requires a folded RNA that serves as a recognition site for eIF3 and 40S subunits (left). Details of this recognition are shown to the right. The binding sites of the 40S subunit and eIF3 are depicted in yellow and blue, respectively. Elements that contact the 40S subunit but do not contribute significantly to binding are shaded in lighter yellow. In green is a portion of the RNA that is critical for binding both the 40S subunit and eIF3. This region includes one of the two folded four-way junctions, both of which are indicated with red circles.

hibit complex formation. Furthermore, the binding efficiencies of these point mutants roughly correlates with their translation initiation activities. Binding specificity was observed at lower potassium ion concentrations (100 mM); however, the concentration of monovalent ion required to maximize specificity and eliminate nonspecific RNA binding to the 40S subunit in vitro (250–300 mM) is somewhat higher than that added to rabbit reticulocyte lysate to achieve maximal HCV IRES-driven translation initiation activity (Borman et al., 1995). This is likely due to the inherent differences in the composition of the two assay systems.

The IRES RNA•40S subunit K_d is 15-fold tighter than that of the IRES RNA•eIF3 complex, and binding of a preformed 40S•eIF3 complex to the IRES RNA is only marginally tighter than binding of the 40S subunit alone. This is consistent with the observation that the RNA elements that bind to the 40S subunit are more highly conserved than the elements that bind eIF3, both in terms of sequence (Smith et al., 1995) and secondary structure (Brown et al., 1992). This suggests that the IRES RNA•40S interaction is more critical to preinitiation complex assembly than the IRES RNA•eIF3 interaction. This idea is further supported by the fact that all mutations that decrease 40S subunit affinity are universally more deleterious to IRES-driven translation initiation activity than a mutation that decreases eIF3 affinity (IIIb_BVDV). Because the HCV IRES RNA•eIF3

does not contribute substantially to 43S particle affinity for the IRES, and eIF3 is generally accepted to be part of the 43S particle by nature of its association with the 40S, the purpose of the specific IRES RNA•eIF3 interaction is not clear. Using qualitative assays, Pestova et al. have shown that eIF3 was not needed to form a complex containing the IRES RNA, the 40S subunit, and met-tRNA•GTP•eIF2, but that eIF3 was needed for subunit joining (Pestova et al., 1998). However, it might have been expected that in quantitative analyses, eIF3 would enhance 40S affinity for the IRES, an effect we do not observe. Taken together, these results seem to suggest that the IRES RNA•eIF3 interaction is superfluous, yet it is highly specific, suggesting there is a purpose for this recognition. It is possible the IRES RNA•eIF3 interaction orients the 40S subunit correctly, prevents IRES RNA binding to 40S subunits that are associated with 60S subunits or activates some other downstream initiation event.

Virtually all of the HCV IRES RNA is involved in 43S particle recruitment (Fig. 7B). The functionally critical IRES RNA•40S interaction involves all three independently folding RNA structural elements: Domain II, JIIIabc, and JIIIef. Binding of eIF3 involves only one of the independently folding junctions (JIIIabc), and two stem-loops that emerge from this junction (IIIa and IIIb). Thus, junction IIIabc is contacting both the 40S subunit and eIF3 and represents a region of intimate intermolecular contact between all members of the ternary complex. Although previous binding assays with HCV IRES RNAs and the 40S subunit suggested that loops IIIa and IIIc do not contribute to 40S subunit binding, our quantitative approach clearly reveals interactions between loops IIIa and IIIc and the 40S subunit (Pestova et al., 1998; Sizova et al., 1998; Kolupaeva et al., 2000). Furthermore, our data do not support the proposal that loop IIIc is involved in eIF3 binding. Domain II, the proposed IIIf pseudoknot element, and domain IV contact the 40S subunit, but must be performing tasks other than providing affinity. In the case of domain II, some reports have shown that this domain is not absolutely essential for HCV IRES driven translation initiation (Wang et al., 1994; Reynolds et al., 1996; Kamoshita et al., 1997; Kolupaeva et al., 2000). Despite this, the apical loop of domain II that contacts the 40S subunit is highly conserved among HCV isolates, the pestiviruses, and GB virus-B, suggesting it plays an important functional role, such as orientating the recruited 43S particle without contributing to affinity (Honda et al., 1999). The proposed pseudoknot might help to position domain IV and the start codon, and domain IV likely unfolds to insert the start codon so that it can pair with initiator tRNA. The presence of these domains that contact the 43S particle but do not contribute to affinity indicate that 43S particle recruitment is a critical step in the path to translation initiation, but other IRES RNA dependent events also must occur.

CONCLUSIONS

Recruitment of the 43S particle by the HCV IRES RNA involves a mechanism distinct from that used by 5′-capped eukaryotic mRNAs or prokaryotic mRNAs. In cap-dependent translation initiation in eukaryotes, recognition of the 43S particle occurs primarily through eIF3, which binds to initiation factor 4G (Fig. 1A). In contrast, HCV recognizes the 43S particle primarily through IRES RNA interaction with the 40S subunit. The direct interaction between the HCV RNA and the 40S subunit is superficially reminiscent of the prokaryotic mechanism of small ribosomal subunit recruitment that involves base pairing between the ribosome and the Shine–Dalgarno sequence. However, HCV RNA binding to the 40S subunit is fundamentally different in that recognition involves three tertiary structural domains of a complex three-dimensional IRES RNA structure that contacts the ribosome in multiple locations. These three IRES RNA tertiary structural domains, unable to bind the 40S subunit individually, act synergistically to tightly and precisely position the 43S particle. The high affinity of the IRES RNA•40S interaction raises the interesting question of how or whether the 40S subunit is released upon initiation of translation.

MATERIALS AND METHODS

Plasmid construction

Plasmids encoding the desired RNA sequences were generated using standard cloning techniques. The construction of plasmids containing wild-type genotype 1b HCV IRES RNA sequence nt 40–372 (p1b35.2), and mutants G266C, G267C, G268C, G(266–268)C, and U288C have been previously described (Kieft et al., 1999). Mutants were generated with either PCR with p1b35.2 as the original template, followed by ligation into the *Eco*R1/*Bam*H1 site of pUC 19, or using Kunkel site-directed mutagenesis (Stratagene). All RNAs contained a hammerhead and hepatitis delta virus ribozyme on the 5′ and 3′ ends, respectively.

RNA transcription, purification, and end labeling

RNA was transcribed in vitro, purified, and 5′ end labeled as previously described (Kieft et al., 1999). To 3′ end label RNA, the 2′-3′ cyclic phosphate was first removed by treatment with T4 polynucleotide kinase (PNK) and calf intestinal phosphatase (CIP) (Cameron & Uhlenbeck, 1977). Briefly, approximately 100 μg of RNA were treated with 20 μL PNK (NEB) and 10 μL CIP (NEB) in 40 mM MES-NaOH, pH 6.0, 10 mM $MgCl_2$, 5 mM DTT, and DEPC-treated water to 100 μL final volume. After incubation at 37 °C for 2–3 h, the reaction was phenol/chloroform extracted, ethanol precipitated, washed with 70% ethanol, dried, and resuspended in 1× TE buffer. RNA was then 3′ end labeled with ^{32}P-pCp and T4 RNA ligase (England & Uhlenbeck, 1978). The RNA labeling reaction contained 5–10 μg 3′ dephosphorylated RNA, 2 μL T4 RNA

ligase buffer (NEB), 4 μL T4 RNA ligase (NEB), 2 μL DMSO, and 8 μL ^{32}P-pCp in 20 μL total volume. The reaction was incubated for 16 h at 16 °C, then purified as described (Kieft et al., 1999).

Isolation and purification of 40S ribosomal subunits and eIF3 from rabbit reticulocyte lysate

40S ribosomal subunits were isolated from rabbit reticulocyte lysate (RRL; Green Hectares) essentially as described (Pestova et al., 1996). Briefly, RRL was thawed on ice in the presence of PMSF and leupeptin and spun in a Beckman ultracentrifuge at 4 °C at 30,000 rpm in a Ti 55.2 rotor for 4 h. The ribosome pellet was resuspended in buffer D (5 mM Tris-HCl, 0.25 M sucrose, 0.1 mM EDTA, 1.0 mM DTT, pH 7.5), using 2 mL of buffer per centrifuge tube. We slowly added 4 M KCl to the polysome suspension to yield a final concentration of 0.5 M, followed by gentle rocking for 30 min, then by ultracentrifugation in a Beckman 55.2 Ti rotor at 4 °C at 40,000 rpm for 4 h. The 0.5 M KCl ribosomal salt wash (0.5 M RSW) supernatant was decanted and used to obtain eIF3 (see below). The pellet was resuspended in buffer A (20 mM Tris-HCl, 50 mM KCl, 4 mM $MgCl_2$, 2 mM DTT, pH 7.5) to a concentration of 100 ODU_{260nm}/mL. Puromycin in buffer A was added to a concentration of 1 mM, and the ribosome suspension was incubated for 10 min on ice, then for 10 min at 37 °C, followed by the addition of 4 M KCl to a final concentration of 0.5 M. The ribosome suspension was then layered onto a 10–30% sucrose gradient in buffer B (20 mM Tris-HCl, 0.5 M KCl, 3 mM $MgCl_2$, 2 mM DTT, pH 7.5) and spun at 22,000 rpm in a Beckman SW28 rotor at 4 °C for 17 h. The 40S subunits were recovered by fractionating the gradient and detecting the absorbance at 280 nm. Fractions containing the 40S subunit were pooled, concentrated, and exchanged into buffer C (0.25 M sucrose, 20 mM Tris-HCl, pH 7.5, 10 mM KCl, 1 mM $MgCl_2$, 1 mM DTT, 0.1 mM EDTA) using Centricon 50 spin concentrators (Amicon) and stored at −20 °C. Concentration of 40S subunits was determined by spectrophotometry, using the conversion 1 ODU_{260nm} = 50 pmol. The concentration of 40S subunits capable of binding the IRES RNA (active concentration) was determined using a stoichiometric filter binding assay. SDS-PAGE analysis verified the absence of any eIF3 contaminants.

eIF3 was isolated from the 0.5 M RSW using a modification of previously published techniques (Benne & Hershey, 1976; Chaudhuri et al., 1997). The solution was brought to 40 mM Tris-HCl, pH 7.5 by addition of 1 M Tris-HCl. While stirring on ice, ammonium sulfate was added slowly to 40%, then the solution was stirred on ice for an additional 30 min. The precipitate was collected by centrifugation at 12,000 rpm for 20 min in an SS-34 rotor, then resuspended in buffer F (20 mM Tris-HCl, pH 7.6, 100 mM KCl, 0.2 mM EDTA, 1 mM DTT) + 5% glycerol. This was loaded directly onto a 15–30% sucrose gradient in buffer F + 5% glycerol and centrifuged for 20 h at 25,000 rpm at 4 °C in a SW27 rotor. Fractions were collected from the gradient, monitoring the absorbance at 280 nm. The location of the eIF3 fraction was determined by SDS-PAGE (about one-third to one-half way into the gradient). eIF3-containing fractions were dialyzed overnight against buffer F + 10% glycerol, purified on a Mono-Q anion exchange column with a 100–500 mM KCl linear gradient in buffer F + 10% glycerol. The eIF3 eluted near 400 mM KCl, and was verified using SDS-PAGE. The complex was concentrated in Centricon-50 spin concentrators and stored in buffer F + 35% glycerol at −20 °C. Concentration was determined by using the absorbance at 280 nm: conversion 1 mg/mL eIF3 yields an absorbance of 1.7. We used a stoichiometric filter binding assay to determine the concentration of active eIF3. SDS-PAGE confirmed the absence of any ribosomal subunit or initiation factor contaminants.

Binding reactions

To generate IRES RNA complexes with eIF3, 40S subunit, or 40S•eIF3, end-labeled RNA was annealed by heating to 75 °C for 1 min then cooled to room temperature. RNA was then added to a tube containing folding/binding buffer (20 mM Tris-HCl, 100 mM potassium acetate, 200 mM KCl, 2.5 mM $MgCl_2$, 1 mM DTT). For 40S•eIF3 binding, the 40S•eIF3 complex was assembled by combining of stoichiometric amounts of each and incubating at 37 °C for 15 min. 40S, eIF3, or 40S•eIF3 was serially diluted immediately before use and then added to the reactions (final volume of reaction was 50 μL). These were incubated at 37 °C for 15–30 min before application to the filter; longer incubation times did not change the measured K_d. All measurements were performed in parallel with wild-type IRES RNA as an internal standard. Reported values are the average of at least three repetitions with standard error.

Filter binding

Filter binding was accomplished using a series of three filters. From top to bottom: a 0.45 μm Tuffryn filter (Gelman) designed to detect aggregates (none were detected), a nitrocellulose filter, and a charged nylon filter. The filters were presoaked in 1× binding buffer, assembled in a dot blot apparatus, and the reactions were added directly with applied vacuum. The filters were then removed, dried, and visualized on a Phosphorimager (Molecular Dynamics). To determine the apparent K_d, the data was fit to a Langmuir isotherm described by the equation $\Theta = [P]/[P] + K_d$ where Θ is fraction RNA bound and [P] is either 40S subunit or eIF3 concentration.

Modification interference

RNA to be used in modification interference was 3′ end labeled and purified (see above). To modify RNA with DEPC, 9 μL labeled RNA (>1,000,000 cpm), and 10 μg tRNA was added to 200 μL DEPC reaction buffer (50 mM sodium acetate, 1 mM EDTA, pH 4.5) and chilled on ice before adding 5 μL DEPC and incubating to 90 °C for 1 min. The reaction was quenched with 50 μL of cold 1.5 M sodium acetate, pH 5.4, and 700 μL cold ethanol. To modify RNA with hydrazine, the labeled RNA was dried in a speed-vac with 10 μg tRNA. The RNA pellet was resuspended in 10 μL of 50:50 hydrazine:water and incubated on ice for 10 min, then quenched with 300 μL of cold 0.3 M sodium acetate, pH 5.4, and 750 μL cold ethanol. Modified RNA was pelleted, resuspended in 0.3 M sodium acetate, and ethanol precipitated a

second time, then washed with 70% ethanol and dried. The modified RNA was then used in binding reactions as described above. The concentration of RNA was kept low enough to remain below the measured K_d, and concentrations of 40S subunit or eIF3 were used to achieve approximately 0.5 fraction bound. Binding reactions were applied to a nitrocellulose filter and then the filter was soaked in 400 mL 0.5 M sodium acetate, pH 5.2, 0.1% SDS, with 5 μL 100 mg/mL proteinase K for 1 h at room temperature, followed by 16 h at 4 °C. After elution, 1 μg tRNA was added and the solution was phenol:chloroform extracted. RNA was precipitated with 1 mL cold ethanol, pelleted, washed with 70% ethanol, and dried. To cleave the RNA at modified sites, 20 mL of fresh aniline buffer (1 M aniline, 1 M acetic acid, pH 4.5) was added to the tube with the RNA pellet and incubated in the dark at 60 °C for 20 min. Aniline cleavage reactions were quenched with 5 mL 3 M sodium acetate pH 5.2 and 75 mL cold ethanol, pelleted, resuspended in 100 mL 0.5 M sodium acetate, pH 5.3, precipitated with 300 mL ethanol, pelleted, washed with 70% ethanol, and dried. RNA was resuspended in 10 mL 7 M urea/1 mM EDTA and electrophoresed on 10% denaturing polyacrylamide gels.

RNase T1 probing

Labeled RNA was annealed as described above, then was added to a tube containing buffer (final concentration 30 mM HEPES, pH 7.5), and desired salt to a volume of 5 mL, then incubated at 37 °C for 5 min to achieve folding equilibrium. A molar excess of 40S subunit was added, and the reaction was incubated at 37 °C for another 15 min. To this, 1 μL of 0.1 U/mL RNase T1 (Boehringer Mannheim) was added and reactions were incubated for 7 min at 37 °C, then quenched by addition of 10 μL DEPC-treated water and 20 μL phenol. After phenol extraction, the reaction was chloroform extracted, ethanol precipitated, washed with 70% ethanol, dried, resuspended in 10 mL 7 M urea/1 mM EDTA, and resolved on 10% polyacrylamide gels. Gels were dried and visualized with a phosphorimager.

Thiophosphate footprinting

To achieve 5% incorporation of the phosphorothioate linkage, α-thio-NTP was added at 0.25 mM final concentration to transcription reactions that contained 5 mM unmodified NTPs (Ortoleva-Donnelly et al., 1998). RNA was purified, concentrated, and either 3′ or 5′ end labeled, then bound to 40S subunit as described for T1 footprinting, above. Cleavage was initiated by the addition of an I_2/ethanol solution to yield a final concentration of 1 mM. The reactions were quenched after 1 min on ice with 2 mL 100 mM thiourea, 20 μL DEPC-treated water and 40 μL phenol. Reactions were resolved by gel electrophoresis and quantitated on a phosphorimager. The protection factors were calculated by comparing the intensity of bands in the absence and presence of bound 40S subunit. Each of the 4 nt were analyzed individually, both 5′ and 3′ end labeling were used, and multiple electrophoretic run times allowed mapping of the entire backbone to nucleotide resolution. Protection factors that were more than one standard deviation from the average on multiple experimental repetitions were assigned as part of the footprint.

Coupled in vitro transcription and translation

The translation initiation efficiencies of U264A, U265A, G266C, G267C, G269C, G(266-269)C, and U228C were previously reported (Kieft et al., 1999). For all others, bicistronic plasmid DNA for use in in vitro translation assays was generated by first assembling a cassette vector containing the *Firefly* (FLUC) and *Renilla* (RLUC) luciferase genes as cistrons 1 and 2, respectively. Plasmid pT7BF(1B/408)R3-13 is essentially identical to plasmid T7BR(1B/408)P7-5 (Jubin & Murray, 1998) except that the respective luciferase reporters have been switched. Briefly, pGL3-control (Promega) containing the firefly luciferase gene was restricted with *Nco*I and *Xba*I and inserted into the same sites in the vector pT7Blue-2 (Novagen). Synthetic DNA oligonucleotides that contained an internal *Bst*BI restriction site were annealed (5′-CGGCACTT CGAATTCG-3′ and 5′-GATCCGAATTCGAAGTGCCGACGT-3′) and inserted into the *Aat*II and *Bam*HI restriction sites in pK1BE2-1 (Kieft et al., 1999). Plasmid RL-Null (Promega) containing the *renilla* luciferase (RL) gene was restricted with *Bst*BI and *Bam*HI and inserted into the modified pK1BE2-1 cut with the same. This IRES-RL plasmid was subsequently restricted with *Ehe*I, then *Bam*HI/*Klenow*, and inserted into pT7BFL restricted with *Xba*I followed by *Klenow* treatment. Mutations were created by swapping *Sma*I fragments from plasmids used to produce in vitro RNAs described above into pT7BF(1B/408)R3-13 restricted with the same. In vitro transcription and translation reactions were carried out using the TNT coupled transcription/translation system (Promega). Duplicate reaction mixtures (25 μL) were assembled containing 19.5 μL of rabbit reticulocyte lysate master mix, 0.5 μL of methionine (1 mM), and 5.0 μL of purified plasmid DNA (0.1 μg/μL). Following the addition of reaction components, samples were analyzed for both FLUC and RLUC reporter activated using the Dual-Luciferase reporter assay system (Promega) according to the manufacturer's instructions and quantitated with a luminometer (Dynex ML5000). The relative translational efficiency in mutational analysis experiments was determined by comparing RL/FL ratios of mutation samples to wild-type IRES.

ACKNOWLEDGMENTS

The authors wish to thank C. Hellen for a 40S subunit isolation protocol. We also thank R. Batey, P. Adams, and J. Cate for critical reading of this manuscript, and S. Lemon, R. Rijnbrand, J. Lau, B. Baroudy, and members of the Doudna laboratory for insightful discussions.

Received September 1, 2000; returned for revision October 27, 2000; revised manuscript received November 2, 2000

REFERENCES

Ali N, Siddiqui A. 1995. Interaction of polypyrimidine tract-binding protein with the 5′ noncoding region of the hepatitis C virus RNA genome and its functional requirement in internal initiation of translation. *J Virol 69*:6367–6375.

Ali N, Siddiqui A. 1997. The La antigen binds 5′ noncoding region of the hepatitis C virus RNA in the context of the initiator AUG codon and stimulates internal ribosome entry site-mediated translation. *Proc Natl Acad Sci USA 94*:2249–2254.

Benne R, Hershey JW. 1976. Purification and characterization of

initiation factor IF-E3 from rabbit reticulocytes. *Proc Natl Acad Sci USA 73*:3005–3009.
Borman AM, Bailly JL, Girard M, Kean KM. 1995. Picornavirus internal ribosome entry segments: Comparison of translation efficiency and the requirements for optimal internal initiation of translation in vitro. *Nucleic Acids Res 23*:3656–3663.
Brown ES, Zhang H, Ping LH, Lemon SM. 1992. Secondary structure of the 5′ nontranslated regions of hepatitis C virus and pestivirus genomic RNAs. *Nucleic Acids Res 20*:5041–5045.
Buratti E, Tisminetzky S, Zotti M, Baralle FE. 1998. Functional analysis of the interaction between HCV 5′ UTR and putative subunits of eukaryotic initiation factor eIF3. *Nucleic Acids Res 26*:3179–3187.
Cameron V, Uhlenbeck OC. 1977. 3′-Phosphatase activity in T4 polynucleotide kinase. *Biochemistry 16*:5120–5126.
Celander DW, Cech TR. 1991. Visualizing the higher order folding of a catalytic RNA molecule. *Science 251*:401–407.
Chaudhuri J, Chakrabarti A, Maitra U. 1997. Biochemical characterization of mammalian translation initiation factor 3 (eIF3). Molecular cloning reveals that p110 subunit is the mammalian homologue of *Saccharomyces cerevisiae* protein Prt1. *J Biol Chem 272*:30975–30983.
Christian EL, Yarus M. 1992. Analysis of the role of phosphate oxygens in the group I intron from *Tetrahymena*. *J Mol Biol 228*:743–758.
Conway L, Wickens M. 1989. Modification interference analysis of reactions using RNA substrates. In: Dahlberg JE, Abelson JN, eds. *Methods in enzymology*. San Diego: Academic Press, Inc. pp 369–379.
England TE, Uhlenbeck OC. 1978. 3′-terminal labeling of RNA with T4 RNA ligase. *Nature 275*:560–561.
Fukushi S, Okada M, Kageyama T, Hoshino FB, Katayama K. 1999. Specific interaction of a 25-kilodalton cellular protein, a 40S ribosomal subunit protein, with the internal ribosome entry site of hepatitis C virus genome. *Virus Genes 19*:153–161.
Garcia-Barrio MT, Naranda T, Vazquez de Aldana CR, Cuesta R, Hinnebusch AG, Hershey JW, Tamame M. 1995. GCD10, a translational repressor of GCN4, is the RNA-binding subunit of eukaryotic translation initiation factor-3. *Genes & Dev 9*:1781–1796.
Goss DJ, Rounds DJ. 1988. A kinetic light-scattering study of the binding of wheat germ protein synthesis initiation factor 3 to 40S ribosomal subunits and 80S ribosomes. *Biochemistry 27*:3610–3613.
Hahm B, Kim YK, Kim JH, Kim TY, Jang SK. 1998. Heterogeneous nuclear ribonucleoprotein L interacts with the 3′ border of the internal ribosomal entry site of hepatitis C virus. *J Virol 72*:8782–8788.
Honda M, Beard MR, Ping LH, Lemon SM. 1999. A phylogenetically conserved stem-loop structure at the 5′ border of the internal ribosome entry site of hepatitis C virus is required for cap-independent viral translation. *J Virol 73*:1165–1174.
Honda M, Brown EA, Lemon SM. 1996a. Stability of a stem-loop involving the initiator AUG controls the efficiency of internal initiation of translation on hepatitis C virus RNA. *RNA 2*:955–968.
Honda M, Ping LH, Rijnbrand RC, Amphlett E, Clarke B, Rowlands D, Lemon SM. 1996b. Structural requirements for initiation of translation by internal ribosome entry within genome-length hepatitis C virus RNA. *Virology 222*:31–42.
Jubin R, Murray MG. 1998. Activity screening of bacteria containing Renilla luciferase plasmids. *Biotechniques 24*:185–188.
Kamoshita N, Tsukiyama-Kohara K, Kohara M, Nomoto A. 1997. Genetic analysis of internal ribosomal entry site on hepatitis C virus RNA: Implication for involvement of the highly ordered structure and cell type-specific transacting factors. *Virology 233*:9–18.
Kieft JS, Zhou K, Jubin R, Murray MG, Lau JY, Doudna JA. 1999. The hepatitis C virus internal ribosome entry site adopts an ion-dependent tertiary fold. *J Mol Biol 292*:513–529.
Kolupaeva VG, Pestova TV, Hellen CU. 2000. An enzymatic footprinting analysis of the interaction of 40S ribosomal subunits with the internal ribosomal entry site of hepatitis C virus. *J Virol 74*:6242–6250.
Latham JA, Cech TR. 1989. Defining the inside and outside of a catalytic RNA molecule. *Science 245*:276–282.
Le SY, Sonenberg N, Maizel JV Jr. 1995. Unusual folded regions and ribosome landing pad within hepatitis C virus and pestivirus RNAs. *Gene 154*:137–143.
Merrick WC, Hershey JWB. 1996. The pathway and mechanism of eukaryotic protein synthesis. In: Hershey JWB, Mathews MB, Sonenberg N, eds. *Translational control*. Cold Spring Harbor, New York: Cold Spring Harbor Laboratory Press. pp 31–69.
Odreman-Macchioli FE, Tisminetzky SG., Zotti M, Baralle FE, Buratti E. 2000. Influence of correct secondary and tertiary RNA folding on the binding of cellular factors to the HCV IRES. *Nucleic Acids Res 28*:875–885.
Ortoleva-Donnelly L, Szewczak AA, Gutell RR, Strobel SA. 1998. The chemical basis of adenosine conservation throughout the *Tetrahymena* ribozyme. *RNA 4*:498–519.
Pain VM. 1996. Initiation of protein synthesis in eukaryotic cells. *Eur J Biochem 236*:747–771.
Pestova TV, Hellen CU, Shatsky IN. 1996. Canonical eukaryotic initiation factors determine initiation of translation by internal ribosomal entry. *Mol Cell Biol 16*:6859–6869.
Pestova TV, Shatsky IN, Fletcher SP, Jackson RJ, Hellen CUT. 1998. A prokaryotic-like mode of cytoplasmic eukaryotic ribosome binding to the initiation codon during internal translation initiation of hepatitis C and classical swine fever virus RNAs. *Genes & Dev 12*:67–83.
Pickering JM, Thomas HC, Karayiannis P. 1997. Predicted secondary structure of the hepatitis G virus and GB virus-A 5′ untranslated regions consistent with an internal ribosome entry site. *J Viral Hepat 4*:175–184.
Psaridi L, Georgopoulou U, Varaklioti A, Mavromara P. 1999. Mutational analysis of a conserved tetraloop in the 5′ untranslated region of hepatitis C virus identifies a novel RNA element essential for the internal ribosome entry site function. *FEBS Lett 453*:49–53.
Reynolds JE, Kaminski A, Carroll AR, Clarke BE, Rowlands DJ, Jackson RJ. 1996. Internal initiation of translation of hepatitis C virus RNA: The ribosome entry site is at the authentic initiation codon. *RNA 2*:867–878.
Rijnbrand R, Bredenbeek P, van der Straaten T, Whetter L, Inchauspe G, Lemon S, Spaan W. 1995. Almost the entire 5′ non-translated region of hepatitis C virus is required for cap-independent translation. *FEBS Lett 365*:115–119.
Rijnbrand RC, Lemon SM. 2000. Internal ribosome entry site-mediated translation in hepatitis C virus replication. *Curr Top Microbiol Immunol 242*:85–116.
Sachs AB, Sarnow P, Hentze MW. 1997. Starting at the beginning, middle, and end: Translation initiation in eukaryotes. *Cell 89*:831–838.
Shine J, Dalgarno L. 1974. The 3′-terminal sequence of *Escherichia coli* 16S ribosomal RNA: Complementarity to nonsense triplets and ribosome binding sites. *Proc Natl Acad Sci USA 71*:1342–1346.
Sizova DV, Kolupaeva VG, Pestova TV, Shatsky IN, Hellen CUT. 1998. Specific interaction of eukaryotic translation initiation factor 3 with the 5′ nontranslated regions of hepatitis C virus and classical swine fever virus RNAs. *J Virol 72*:4775–4782.
Smith DB, Mellor J, Jarvis LM, Davidson F, Kolberg J, Urdea M, Yap PL, Simmonds P. 1995. Variation of the hepatitis C virus 5′ noncoding region: Implications for secondary structure, virus detection and typing. *J Gen Virol 76*:1749–1761.
Tang S, Collier AJ, Elliott RM. 1999. Alterations to both the primary and predicted secondary structure of stem-loop IIIc of the hepatitis C virus 1b 5′ untranslated region (5′UTR) lead to mutants severely defective in translation which cannot be complemented *in trans* by the wild-type 5′UTR sequence. *J Virol 73*:2359–2364.
Varaklioti A, Georgopoulou U, Kakkanas A, Psaridi L, Serwe M, Caselmann WH, Mavromara P. 1998. Mutational analysis of two unstructured domains of the 5′ untranslated region of HCV RNA. *Biochem Biophys Res Commun 253*:678–685.
Wang C, Le SY, Ali N, Siddiqui A. 1995. An RNA pseudoknot is an essential structural element of the internal ribosome entry site located within the hepatitis C virus 5′ noncoding region. *RNA 1*:526–537.
Wang C, Sarnow P, Siddiqui A. 1994. A conserved helical element is essential for internal initiation of translation of hepatitis C virus RNA. *J Virol 68*:7301–7307.
Yen JH, Chang SC, Hu CR, Chu SC, Lin SS, Hsieh YS, Chang MF. 1995. Cellular proteins specifically bind to the 5′-noncoding region of hepatitis C Virus RNA. *Virology 208*:723–732.